

### Fission stability diagram of $^{240}\text{Pu}$

F. Garcias, M. Barranco, and H. S. Wio\*

*Departament de Física, Universitat de ses Illes Balears, E-07071 Palma de Mallorca, Spain*

C. Ngô

*Laboratoire National Saturne, F-91191 Gif-sur-Yvette, France*

J. Nemeth

*Institute of Theoretical Physics, Eötvös University, H-1088 Budapest, Hungary*

(Received 9 March 1989)

We have used an axially symmetric deformed Thomas-Fermi model to evaluate the fission barrier of  $^{240}\text{Pu}$  as a function of the quadrupole moment  $Q_2$  for different values of the angular momentum  $L$  and temperature  $T$ . The fission stability diagram of this nucleus is investigated.

In a recent paper,<sup>1</sup> we presented some results for the fission barriers  $B$  of hot rotating nuclei obtained with a deformed Thomas-Fermi (TF) model. The main characteristics of this two-dimensional (2D) model are the following.

(1) It *self-consistently* incorporates the effects of rotation (rigid or hydrodynamical) and temperature.

(2) It uses a realistic Skyrme force, namely SkM\* (Ref. 2) and the *complete* semiclassical expressions for the kinetic and spin-orbit energies up to  $\hbar^2$ .

To improve the surface properties of this  $\hbar^2$  TF Model, an effective Weizsäcker coefficient  $\beta/36$ , with  $\beta=1.6$  for SkM\* instead of the standard  $\beta=1$  value,<sup>3</sup> was used. The results so obtained compare well with the liquid drop model ones for light and medium nuclei,<sup>4</sup> but the barriers for heavy ( $A > 210$ ) nuclei are underestimated.

The purpose of this work is to present detailed results for  $^{240}\text{Pu}$ . This nucleus has been the subject of rather exhaustive studies in the Hartree-Fock (HF) (Refs. 5-7) and TF (Refs. 8 and 9) approximations, but in none of them has the question of how  $B$  evolves with  $L$  and  $T$  simultaneously been addressed. To make quantitative predictions about  $B(L, T)$ , we have to reproduce fairly well the semiclassical  $L=T=0$  barrier.<sup>5</sup> This has led us to use  $\beta=2$  for the Weizsäcker coefficient.

In order to obtain the equilibrium density at given values of  $Q_2=Q_0$  (in barns),  $L$  (in units of  $\hbar$ ), and  $T$  (in MeV), we minimize the quantity

$$\langle F \rangle + \frac{1}{2}\lambda(\langle Q_2 \rangle - Q_0)^2 - \omega L_x, \tag{1}$$

where  $F$  is the free energy. We have imposed axial symmetry around the  $z$  axis and only considered symmetric fission. Rotation was described in the standard rigid body approximation.<sup>10,11</sup>

From bottom to top, Fig. 1 shows the  $T=0$  fission barrier for  $L=0, 20$ , and  $40$ . The critical  $L$  is  $L_{cr} \approx 50$ . No-

tice that at high values of  $L$  (40 in that figure), the rigid rotation is able to yield equilibrium shapes with  $Q_2 \neq 0$ .

Figure 2 shows contour plots of the nuclear density in the  $(r, z)$  cylindrical coordinates plane for the  $L=T=0$  saddle configuration. From outside to inside, the lines correspond to  $\rho=0.03, 0.06, 0.09$ , and  $0.12 \text{ fm}^{-3}$ . One can see that the surface diffuseness depends very little on deformation. Similar plots could be drawn for  $L=20$  and  $40$ .

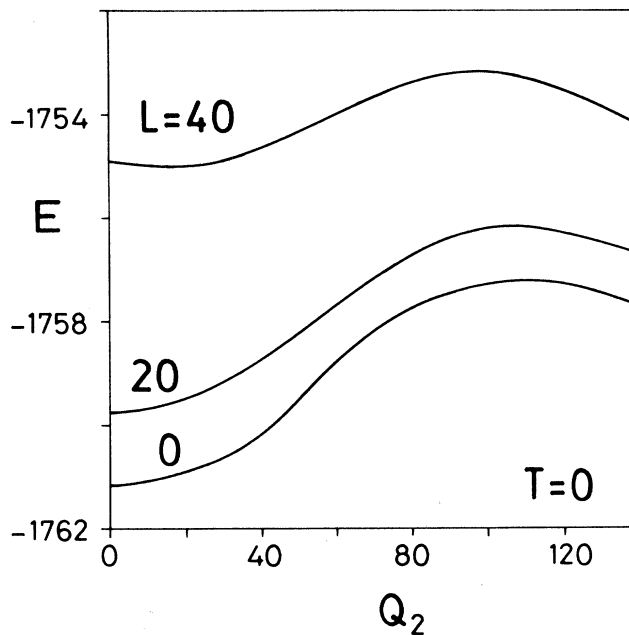


FIG. 1. Fission barriers of  $^{240}\text{Pu}$  for  $L=0\hbar, 20\hbar$ , and  $40\hbar$ . Energies are in MeV and quadrupole moments in barns.

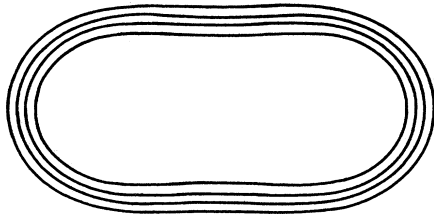


FIG. 2. Contour plots of the  $^{240}\text{Pu}$  density for the saddle configuration at  $L=T=0$ . From outside to inside,  $\rho=0.03, 0.06, 0.09,$  and  $0.12 \text{ fm}^{-3}$ .

The  $\rho=0.14 \text{ fm}^{-3}$  equidensity lines corresponding to the  $L=0, 20,$  and  $40$  saddle configurations at  $T=0$  are represented in Fig. 3 (upper curves). The larger the angular momentum, the more compact the saddle. The  $\rho=0.14 \text{ fm}^{-3}$  equidensity lines corresponding to the  $T=0, 1,$  and  $2 \text{ MeV}$  saddle configurations at  $L=0$  are also shown in this figure (bottom curves). The higher the temperature, the more compact the saddle. It is worth mentioning that these changes in the equidensity lines are not due to morphological changes in  $\rho$  induced by rotational and/or thermal effects (which are rather small), but to the saddle-point displacement induced by the fission energy balance. As an example, at  $T=0, Q_2^s$  (saddle) changes from  $\approx 110$  to  $\approx 90$  barns when  $L$  goes from 0 to 40. At  $L=0, Q_2^s$  changes from  $\approx 110$  to  $\approx 80$  barns when  $T$  goes from 0 to 2 MeV.

Finally, Fig. 4 shows the fission stability diagram  $B(L, T)$  of  $^{240}\text{Pu}$ . Full lines correspond to a cubic spline of the exact calculations and dashed lines to the heuristic

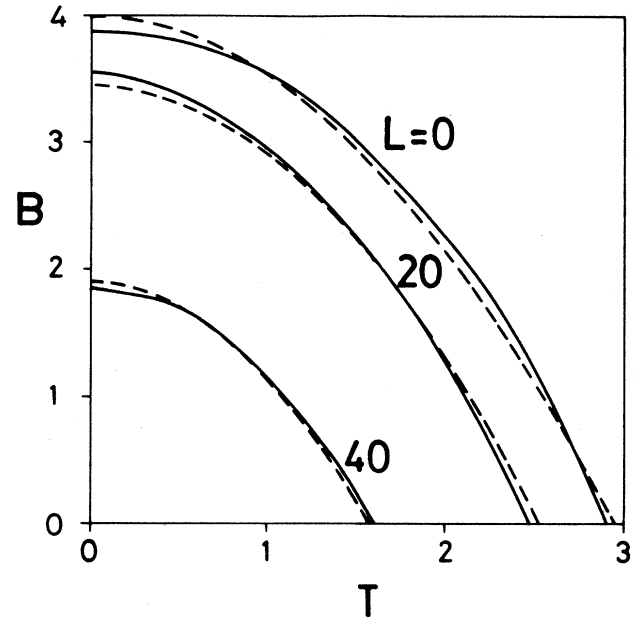


FIG. 4. Evolution of the fission barrier  $B$  (MeV) with angular momentum  $L$  ( $\hbar$ ) and  $T$  (MeV). The dashed lines correspond to the fit given by Eq. (2).

fit

$$B(L, T) = 4.005 - (1.465 \times 10^{-3} L^2 - 3.857 \times 10^{-6} L^3) - (4.610 \times 10^{-1} + 1.892 \times 10^{-4} L^2) T^2 \text{ (MeV)}. \quad (2)$$

From this expression, one may infer that there is little correlation between angular momentum and temperature effects (the  $L^2 T^2$  term is just a small correction). Concerning Fig. 4, we want to point out that the precise way the barriers go to zero with  $T$  is rather uncertain because of the limited numerical accuracy inherent to any 2D calculation.

In conclusion, this axially symmetric self-consistent Thomas-Fermi model allows one to calculate the temperature and angular momentum evolution of the semiclassical fission barrier. For  $^{240}\text{Pu}$  we have found that it vanishes for  $L \approx 50$  at  $T=0$  and for  $T \approx 2.9 \text{ MeV}$  at  $L=0$ . This last  $L=0$  result agrees well with previous estimates.<sup>7</sup> The fission barrier height can be fitted by a simple analytical function of  $L$  and  $T$ .

We are indebted to Xavier Viñas for his contribution to the development of the 2D TF code. This work has been supported by the Comisión Interministerial de Ciencia y Tecnología [CICYT (Spain)], under Grant PB85-0072-C02-00. H.S.W. thanks the Dirección General de Investigación Científica y Técnica [DGICYT (Spain)] for financial support.

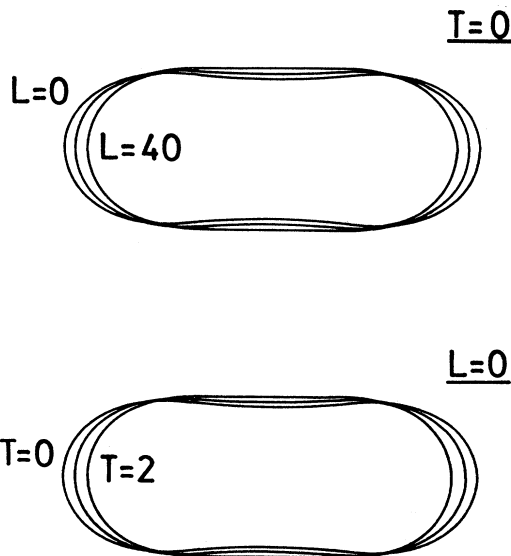


FIG. 3.  $\rho=0.14 \text{ fm}^{-3}$  equidensity lines corresponding to the saddle configurations. Units are MeV for  $T$  and  $\hbar$  for  $L$ .

- \*On leave of absence from Centro Atómico Bariloche, 8400-S.C. Bariloche, Argentina.
- <sup>1</sup>F. Garcias, M. Barranco, J. Nemeth, C. Ngô, and X. Viñas, Nucl. Phys. **A495**, 169 (1989).
- <sup>2</sup>J. Bartel, P. Quentin, M. Brack, C. Guet, and H. B. Håkansson, Nucl. Phys. **A386**, 79 (1982).
- <sup>3</sup>D. A. Kirznits, *Field Theoretical Methods in Many Body Systems* (Pergamon, Oxford, 1967).
- <sup>4</sup>W. D. Myers, *Droplet Model of Atomic Nuclei* (IFI/Plenum, New York, 1977).
- <sup>5</sup>M. Brack and P. Quentin, Nucl. Phys. **A361**, 35 (1981).
- <sup>6</sup>H. Flocard, P. Quentin, D. Vautherin, M. Vénéroni, and A. K. Kerman, Nucl. Phys. **A231**, 176 (1974).
- <sup>7</sup>J. Bartel and P. Quentin, Phys. Lett. **152B**, 29 (1985).
- <sup>8</sup>M. Brack, C. Guet, and H. B. Håkansson, Phys. Rep. **123**, 275 (1985).
- <sup>9</sup>C. Guet, E. Strumberger, and M. Brack, Phys. Lett. **B 205**, 427 (1988).
- <sup>10</sup>S. Cohen, F. Plasil, and W. J. Swiatecki, Ann. Phys. (N.Y.) **82**, 557 (1974).
- <sup>11</sup>A. J. Sierk, Phys. Rev. C **33**, 2039 (1986).